Multi-sensor, Multi-resolution image fusion for Monitoring of Wetlands

Uttam Kumar[1, 2, 3], Anindita Dasgupta[1], Chiranjit Mukhopadhyay[3], N. V. Joshi[1] and T. V. Ramachandra[1, 2, 4]

[1]Energy & Wetlands research Group, Centre for Ecological Sciences,
[2]Centre for Sustainable Technologies,
[3]Department of Management Studies,
[4]Centre for *infrastructure*, Sustainable Transport and Urban Planning,
Indian Institute of Science, Bangalore -560012, India.
Email : uttam@ces.iisc.ernet.in, anindita_dasgupta@ces.iisc.ernet.in, cm@mgmt.iisc.ernet.in, nvjoshi@ces.iisc.ernet.in, cestvr@ces.iisc.ernet.in

Abstract

Wetlands are an essential part of human civilization meeting many crucial needs for life on earth such as drinking water, energy, biodiversity, recreation, and climate stabilizers. Burgeoning populations, intensified human activity, unplanned development, absence of management structures, and lack of awareness about the vital role played by these ecosystems are the important causes that have contributed to their decline and loss. Identifying, delineating, and mapping of wetlands on a temporal scale provide an opportunity to monitor the changes, which is important for natural resource management and planning activities. Temporal RS data coupled with spatial analysis helps in monitoring the status and extent of spatial features. Extracting spatial features such as wetlands (which include lakes, ponds, tanks, marshy areas, etc.) from multi-sensor multi-resolution images acquired from the earth observation satellites helps in monitoring their status including spatial extent, physical, chemical, and ecological aspects. In this work an attempt has been made to evaluate the performance of five image fusion techniques on mutli-sensor multi-resolution remote sensing data. Finally, the optimal fused images were used to carry out the temporal analyses of wetlands in Greater Bangalore using pattern classifier, which indicated decline of 60.83% of wetlands area during 1973-2007 due to increase in built-up area. There were 159 wetlands spread in an area of 2003 ha in 1973 which declined to 93 (both small and medium size) with an area of 918 ha.

Keywords: Multi-resolution, multi-sensor, image fusion, pattern classifier, wetlands.

1. INTRODUCTION

Wetlands are an essential part of human civilization, meeting many crucial needs for life on earth such as drinking water, protein production, energy, fodder, biodiversity, flood storage, transport, recreation, and climate stabilizers. They also aid in improving water quality by filtering sediments and nutrients from surface water. Wetlands play a major role in removing dissolved nutrients such as nitrogen and to some extent heavy metals (Ramachandra, 2002). They are becoming extinct due to manifold reasons, including anthropogenic and natural processes. Burgeoning population, intensified human activity, unplanned development, absence of management structures, lack of proper legislation, and lack of awareness about the vital role played by these ecosystems are the important causes that have contributed to their decline and loss. Identifying, delineating, and mapping of wetlands on a temporal scale provide an opportunity to monitor the changes, which is important for natural resource management and planning activities (Ramachandra, Kiran, & Ahalya, 2002). Temporal RS data coupled with spatial analysis helps in monitoring the status and extent of spatial features.

Extracting spatial features such as wetlands (which include lakes, ponds, tanks, marshy areas, etc.) from temporal RS data helps in monitoring their status including spatial extent, physical, chemical, and ecological aspects. Traditional approaches are digitizing through visual investigation, applying a density slicing method or an edge detection method to a single band, and classification using multiple bands (Kevin & El Asmar, 1999). However, extraction of features in now possible with multi-sensor multi-resolution images acquired from the earth observation satellites.

Earth observation satellites provide data covering different portions of the electromagnetic spectrum at different spatial, spectral, temporal and radiometric resolutions giving a more complete view of the observed objects. However, two major factors limit sensor's ability to collect high spatial resolution (HSR), Multispectral (MS) data. First, the incoming radiation energy to sensor is limited by optics size. Second, the data volume to be collected and stored by the sensor increases exponentially with HSR. With physical and technological constraints, some satellite sensors supply the spectral bands needed to distinguish features spectrally but not spatially, while other satellite sensors supply the spatial resolution for distinguishing features spatially but not spectrally. For many applications, combination of data from multiple sensors provides more comprehensive information. Thus, satellites such as QuickBird, IKONOS, IRS bundle a 1:4 ratio while Landsat and SPOT bundle a 1:2 ratio of a HSR Panchromatic (PAN) band and low spatial resolution (LSR) MS bands in order to support both colour and best spatial resolution while minimising on-board data handling needs. A critical consideration is how to integrate spatial information present in the PAN image but missing from the LSR MS data. Therefore, for full exploitation of increasingly sophisticated multi-source data, advanced analytical or numerical image fusion techniques are required.

Image fusion refers to combining the geometric detail of a HSR PAN image and the spectral information of a LSR MS image to produce a final image with the highest possible spatial information content while preserving good spectral information quality.

It describes a group of methods and approaches using multi-source data of different nature to increase quality of information contained in the data. Fused images provide increased interpretation capabilities, more reliable results as data with different characteristics are combined, reduces ambiguity, improves reliability, improves classification, substitutes missing information and are also used for feature extraction, flood monitoring, ice/snow monitoring, geological applications, etc.

However, for a particular application, it is necessary to have apt spectral and spatial resolution, which is a constrain by availability. Availability depends on the satellite coverage, operational aspects, atmospheric constraints such as cloud cover, economic issues, suitable fusion level, geometric model, ground control points, re-sampling method etc. Considering all these aspects, an attempt has been made to evaluate the performance of five image fusion techniques such as SFIM (Smoothing Filter), COS (Component Substitution), High Pass (HP) Fusion, High Pass (HP) Filter and High Pass Modulation (HPM) when applied on different resolution ratios (PAN and MS obtained from different sensors), such as (i) Fusion of 1:4 resolution ratio (IRS PAN 5.8 m + LISS-III MS 23.5 m), (ii) Fusion of 1:2 resolution ratio (Landsat ETM + PAN 15 m + MS 30 m), (iii) Fusion of 1:50 resolution ratio (IRS PAN 5 m + MODIS 250 m), (iv) Fusion of 1:100 resolution ratio (IRS PAN 5 m + MODIS 500 m), (v) Fusion of 1:250 resolution ratio (IKONOS PAN 1 m + MODIS 250 m), and (vi) Fusion of 1:500 resolution ratio (IKONOS PAN 1 m + MODIS 500 m).

The main objectives of this study are

(i) to find out the best technique for fusing images of different resolution ratios in order to achieve both high spatial and high spectral resolutions.
(ii) to carry out spatial and temporal analysis of wetlands (change during the period 1973-2007) in Greater Bangalore through pattern classifies to understand responsible causal factors and the likely implication of these dynamics.

The paper is organised as follows. Section 2 discusses data followed by methods in section 3. Results and discussion is presented in section 4 followed by concluding remarks in section 5.

2. DATA

The details of remote sensing data used for each resolution ratio are listed in Table 1.

Table Error! No text of specified style in document.**: Details of different resolution ratios used in image fusion**

Resolution ratio	Sensor	Spatial Resolution	Spectral Resolution	Size	Data of acquisition
1:4	IRS PAN	5.8 m (resampled to 6 m)	1 band	4000 x 4000	1-Dec-2002
	IRS LISS-III MS	23.5 m (resampled to 24 m)	3 bands	1000 x 1000	25-Dec-2002
1:2	ETM+ PAN	15 m	1 band	80 x 108	22-Nov-2004
	ETM+ MS	30 m	6 bands (excluding thermal band)	40 x 54	22-Nov-2004
1:50	IRS PAN 5.8 m (resampled to 5 m)	5.8 m (resampled to 5 m)	1 band	5000 x 5000	1-Dec-2002
	MODIS	250 m	7 bands	100 x 100	19 to 26-Dec-2002
1:100	IRS PAN	5.8 m (resampled to 5 m)	1 band	5000 x 5000	1-Dec-2002
	MODIS	500 m	7 bands	50 x 50	19 to 26-Dec-2002
1:250	IKONOS PAN	1 m	1 band	10000 x 10000	23-Feb-2004
	MODIS	250 m	7 bands	40 x 40	18 to 25-Feb-2004
1:500	IKONOS PAN	1 m	1 band	10000 x 10000	23-Feb-2004
	MODIS	500 m	7 bands	20 x 20	18 to 25-Feb-2004

3. METHODS

3.1 Image Fusion Techniques

Five best image fusion techniques based on literature review and comparative evaluation were used. These techniques are smoothing Filter- SFIM (Bharath et al., 2009), COS (Component Substitution) (Kumar et al., 2011), High Pass Fusion-HPF (Kumar et al., 2009a), High Pass Filter-HPF (Kumar et al., 2009b) and High Pass Modulation-HPM (Kumar et al., 2009b).

3.2 Methods of validation

The performance of the image fusion techniques were analysed qualitatively and quantitatively by visual interpretation and correlation coefficient (CC) that is often used as a similarity metric in image fusion. However, CC is insensitive to a constant gain and bias between two images and does not allow subtle discrimination of possible fusion artifacts (Aiazzi et al., 2002). In addition, a universal image quality index (UIQI) (Wang et al., 2005) is used to measure the similarity between two images. UIQI is designed by modelling any image distortion as a combination of three factors: loss of correlation, radiometric distortion, and contrast distortion given by:

$$Q = \frac{\sigma_{AB}}{\sigma_A \sigma_B} \cdot \frac{2\mu_A \mu_B}{\mu_A^2 + \mu_B^2} \cdot \frac{2\sigma_A \sigma_B}{\sigma_A^2 + \sigma_B^2} \quad (1)$$

The first component is the CC for A (original MS band) and B (fused MS band). The second component measures how close the mean gray levels of A and B is, while the third measures similarity between the contrasts of A and B. The dynamic range is [-1, 1]. If two images are identical, the similarity is maximal and equals 1. In addition, minimum (min), maximum (max), and sd of the original and fused bands were also analysed. These are the most commonly used indices/measures found in literature that provide robust statistics for validating the fused images with the original reference images at the original image resolution.

3.3 Pattern classifier

A pattern classifier (K-Means Clustering) was used to delineate the wetlands (Ramachandra and Kumar, 2008) from the fused spectral bands for the different sensor data.

4. RESULTS AND DISCUSSION

4.1 Fusion of 1:4 resolution ratio (IRS PAN 5.8 m + LISS-III MS 23.5 m)

The five image fusion techniques were applied on IRS PAN and LISS-III MS bands (Table 1) as shown in Figure 2. A 5 x 5 filter was used in SFIM, HP Fusion, HP Filter and HPM. A linear regression of IRS PAN and LISS-III MS sensor Spectral Response Function (SRF) (values were obtained from Space Application Centre (SAC), Ahmedabad, India) is carried out (Figure 1). The regression coefficient $\overline{C}$ is derived for each MS band. ($C_1 = 0.49621700$, $C_2 = 0.48983800$ and $C_3 = 1.52746000$) for IRS-1D LISS-III MS 3 bands.

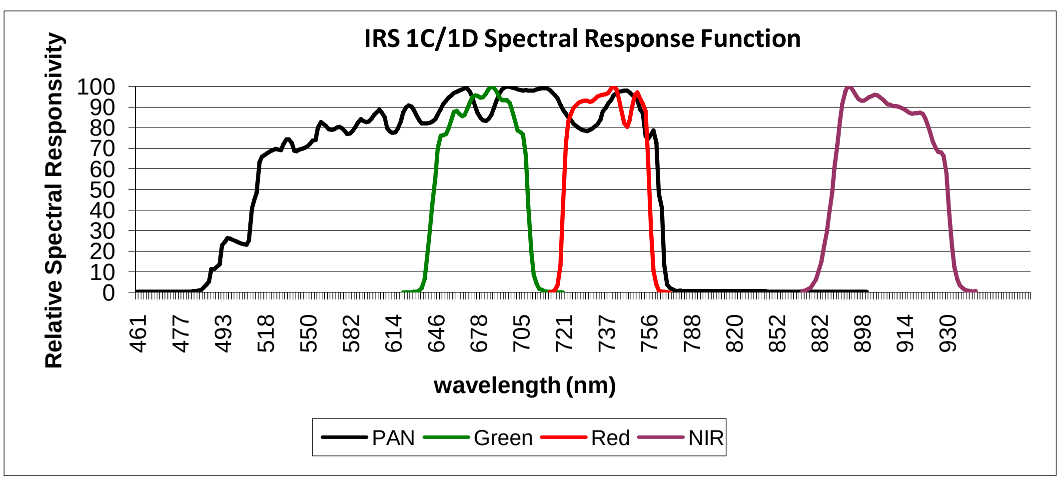

Figure 1: Spectral response pattern of IRS 1C/1D PAN and LISS-III MS bands.

$r = 4.41626816$ and $\overline{W}$ for IRS 1D is ($W_1 = 0.6114$, $W_2 = 0.5945$, and $W_3 = 0.7686$).

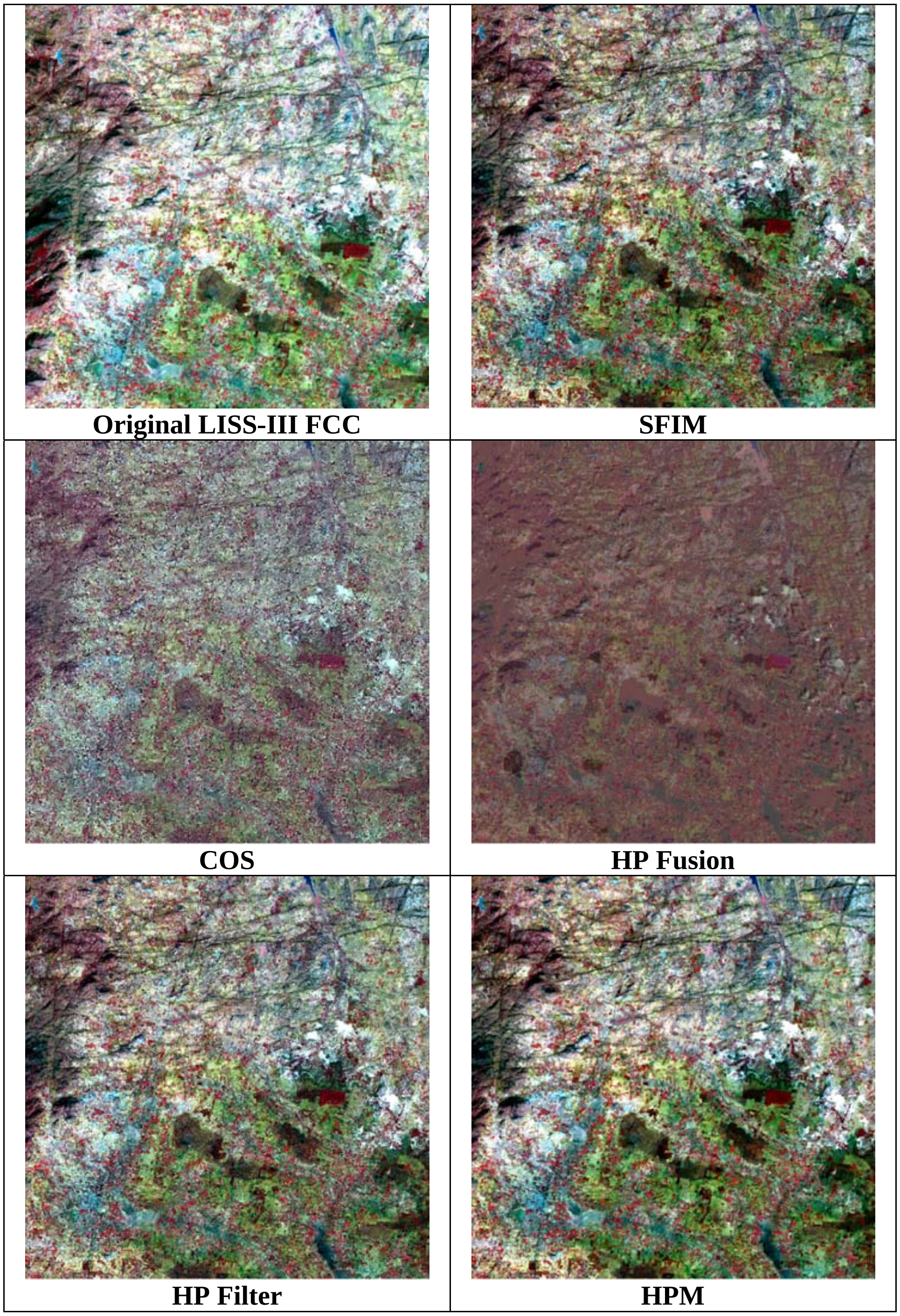

Figure Error! No text of specified style in document.**: IRS LISS-III MS + PAN fused outputs at 6 m from 5 best performing techniques.**

It is apparent from Figure 2 that SFIM, HP Filter and HPM have produced good quality images. COS, and especially HP Fusion have produced significant colour distortion. The UIQI values, CC of PAN with synthetic PAN, and CC between original and degraded fused images closest to 1 and min, max, and sd values closer to original band values are highlighted in Table 2, 3 and 4.

Table Error! No text of specified style in document.**: UIQI measurements of the similarities between original IRS LISS-III MS and fused bands and correlation between IRS PAN and simulated PAN**

Sl. No.	Algorithms	Green	Red	NIR	CC (*p* value < 2.2e-16)
1	SFIM	0.95	0.97	0.93	-
2	COS	0.03	0.05	0.01	**1**
3	HP Fusion	0.61	0.65	0.61	-0.92
4	HP Filter	0.88	0.92	0.85	0.95
5	HPM	**0.99**	**0.99**	**0.99**	0.95

Table Error! No text of specified style in document.**: Minimum and maximum values of the IRS LISS-III MS original and fused bands**

Sl. No.	Algorithms	Minimum			Maximum		
		Green	Red	NIR	Green	Red	NIR
	Original bands	42	28	26	252	247	187
1	SFIM	35	26	25	261	**247**	195
2	COS	-217	-215	-285	465	456	512
3	HP Fusion	-4.8	-19.8	-14.6	174	167	135
4	HP Filter	-13	-17	-1	**257**	244	**194**
5	HPM	**42**	**28**	**26**	264	256	197

Table Error! No text of specified style in document.**: Standard deviation and correlation values between the IRS LISS-III MS original and fused bands**

Sl. No.	Algorithms	Standard deviation			CC (*p* value < 2.2e-16)		
		Green	Red	NIR	Green	Red	NIR
	Original bands	13	17	12	-	-	-
1	SFIM	14	17	13	0.95	0.97	0.93
2	COS	88	87	109	0.34	0.37	0.29
3	HP Fusion	11	13	10	0.82	0.88	0.78
4	HP Filter	15	18	14	0.88	0.92	0.85
5	HPM	**13**	**17**	**12**	**0.99**	**0.99**	**0.99**

From the above fusion quality measures, it is evident that HPM retained most of the statistical properties of IRS LISS-III MS fused bands and is most suitable technique for merging IRS MS and PAN images.

4.2 Fusion of 1:2 resolution ratio (Landsat ETM + PAN 15 m + MS 30 m)

Linear regression of Landsat ETM+ PAN and MS sensor SRF (http://landsathandbook.gsfc.nasa.gov/handbook/handbook_htmls/chapter8/chapter8.html) is shown in Figure 3. Regression coefficient are $C_1 = 1.05382$, $C_2 = 1.01807$, $C_3 = 1.28137$, $C_4 = 0.91850$, $C_5 = 1.67559$ and $C_7 = 1.35889$ for MS 6 bands (except band 6 - thermal band); $r = 0.711068$; $\overline{W}$ is ($W_1 = 0.124744$, $W_2 = 0.109538$, $W_3 = 0.106031$, $W_4 = 0.103585$, $W_5 = 0.164548$ and $W_7 = 0.184194$).

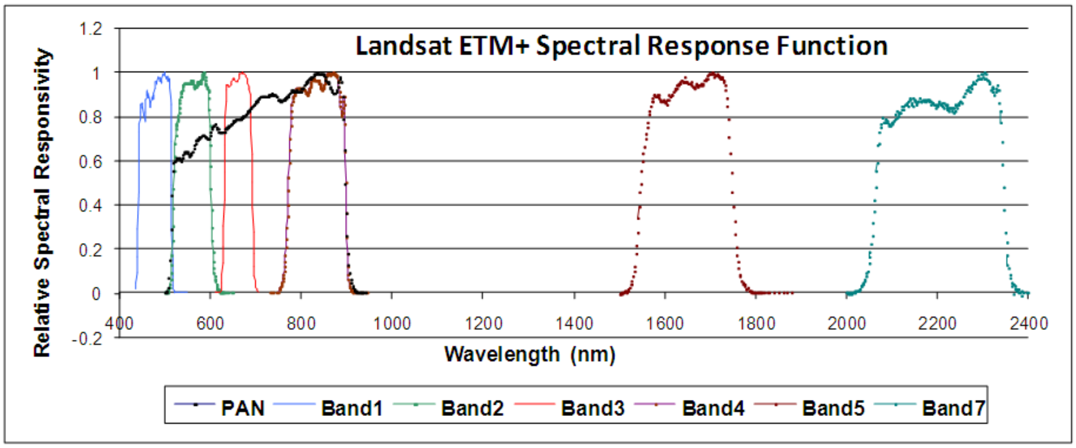

Figure 3: Spectral response pattern of Landsat ETM+.

The five image fusion techniques were applied on Landsat ETM+ PAN and MS bands as shown in Figure 4. Statistical properties of the fused images were assessed as per Table 5-9.

Table Error! No text of specified style in document.**: UIQI measurements of the similarities between Landsat ETM+ original and the fused bands and correlation between Landsat ETM+ original and simulated PAN**

Sl. No.	**Algorithms**	**Blue**	**Green**	**Red**	**NIR**	**MIR-1**	**MIR-2**	**CC** (*p* value = 2.2e-16)
1	SFIM	0.6756	0.8183	0.9136	0.8868	0.9280	0.9373	-
2	COS	**0.99**	**0.99**	**0.99**	**0.99**	**0.98**	0.98	**1**
3	HP Fusion	0.5764	0.6349	0.7405	0.6873	0.8003	0.7600	0.34
4	HP Filter	0.8334	0.8900	0.9595	0.8971	0.9755	**0.9990**	0.76
5	HPM	0.75	0.84	0.93	0.90	0.96	0.95	0.76

Table 6: Minimum values of the Landsat ETM+ MS original and fused bands (1:2)

Sl. No.	**Algorithms**	**Minimum**					
		Blue	Green	Red	NIR	MIR-1	MIR-2

	Original bands	57	40	27	27	31	14
1	SFIM	32	25	20	16	17	12
2	COS	**54**	**38**	21	22	14	1
3	HP Fusion	39	26	19	17	27	9
4	HP Filter	42	25	18	14	18	8
5	HPM	39	25	**27**	**22**	**28**	**14**

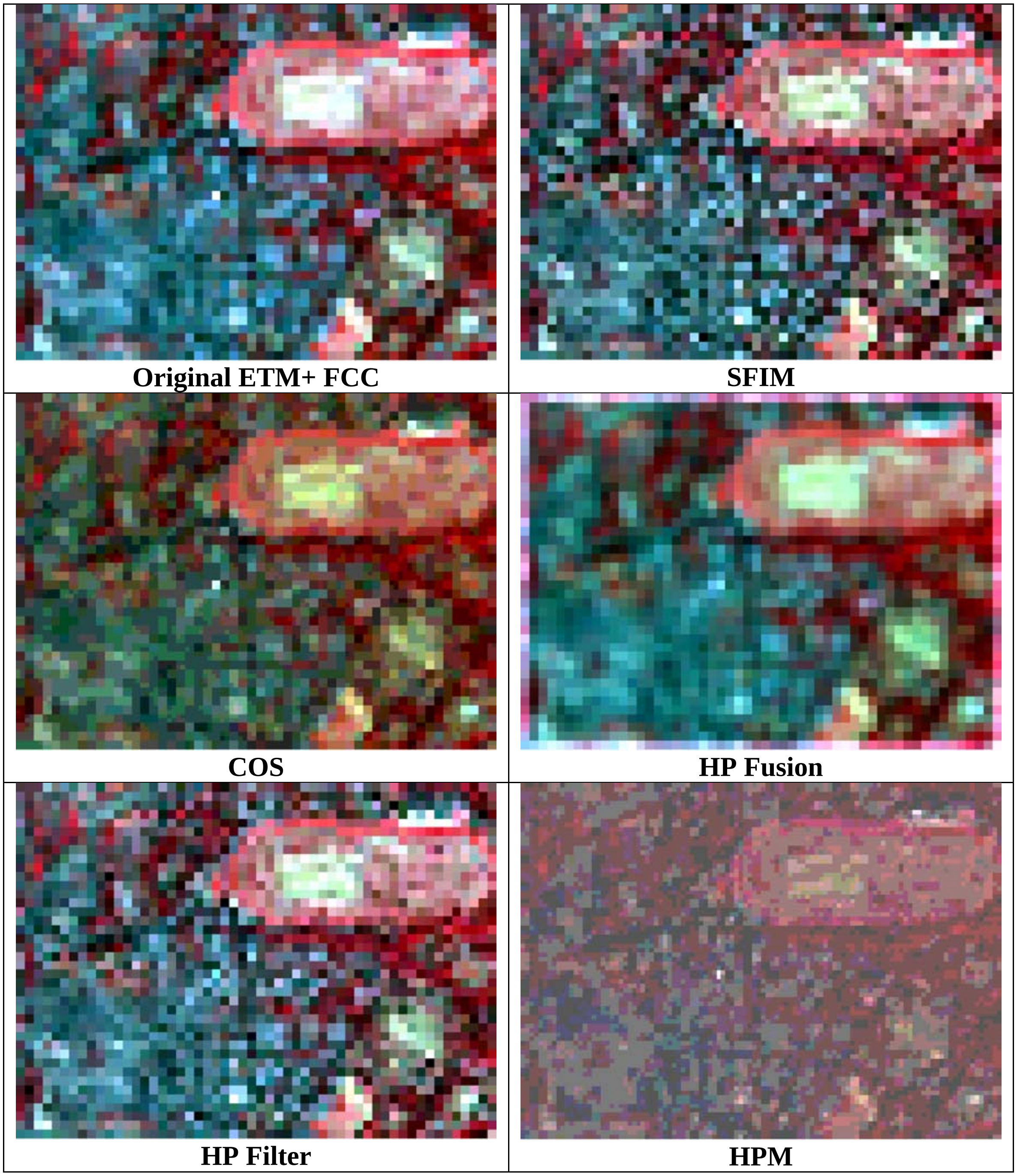

Figure Error! No text of specified style in document.**: Landsat ETM+ PAN + MS fused outputs at 15m from 5 best performing techniques.**

Table 7: Maximum values of the Landsat ETM+ MS original and fused bands (1:2)

Sl. No.	Algorithms	Maximum					
		Blue	Green	Red	NIR	MIR-1	MIR-2
	Original bands	144	139	168	102	233	200
1	SFIM	305	290	349	184	372	381
2	COS	154	146	**179**	**105**	269	227
3	HP Fusion	88	81	108	82	143	121
4	HP Filter	**152**	**145**	186	115	**237**	**203**
5	HPM	167	160	242	127	272	238

Table Error! No text of specified style in document.**: Standard deviation of the Landsat ETM+ MS original and fused bands (1:2)**

Sl. No.	Algorithms	Standard deviation					
		Blue	Green	Red	NIR	MIR-1	MIR-2
	Original bands	10	13	22	14	29	26
1	SFIM	15	17	26	16	32	29
2	COS	**11**	**14**	25	**14**	36	32
3	HP Fusion	8	9	15	10	20	17
4	HP Filter	13	15	**24**	15	**30**	**28**
5	HPM	15	17	26	16	33	29

Table Error! No text of specified style in document.**: Correlation values between the Landsat ETM+ MS original and fused bands (1:2)**

Sl. No.	Algorithms	**CC** (*p* value < 2.2e-^{16})					
		Blue	Green	Red	NIR	MIR-1	MIR-2
1	SFIM	0.73	0.84	0.92	0.90	0.93	0.94
2	COS	**0.99**	**0.99**	**0.99**	**0.99**	**0.99**	0.99
3	HP Fusion	0.63	0.73	0.87	0.79	0.92	0.89
4	HP Filter	0.85	0.90	0.96	0.90	0.98	**1.00**
5	HPM	0.80	0.87	0.94	0.91	0.94	0.95

From the fusion quality assessment it is apparent that HPM has significantly distorted the colour. COS is best for fusing 1:2 Landsat ETM+ PAN and MS bands. A reason for better performance of COS than others could be the well defined spectral response function of Landsat ETM+, where the wavelength of PAN band (0.520-0.900 μm) completely encompasses the VIS (visible - G, R) and NIR bands (0.525-0.900

μm). Note that in case of IRS sensor, PAN wavelength only encompasses the G and R bands, and so the same technique could not perform well.

4.3 Fusion of 1:50 resolution ratio (IRS PAN 5 m + MODIS 250 m)

The five image fusion techniques were applied on IRS PAN at 5 m and MODIS 7 bands at 250 m. SRF of IRS 1C/1D PAN and MODIS 7 bands is shown in Figure 5.

$C_1 = 0.1184$, $C_2 = 0.0855$, $C_3 = 0.1315$, $C_4 = 0.1241$, $C_5 = 0.0065$, $C_6 = 0.8947$ and $C_7 = 0.0087$; $r = 0.2729$; $\overline{W}$ is ($W_1 = 1.6209$, $W_2 = 2.3103$, $W_3 = 2.0341$, $W_4 = 2.0009$, $W_5 = 2.2122$, $W_6 = 2.2519$ and $W_7 = 2.4628$).

The original, fused images and statistical properties of the fused bands (not shown here due to space constraint) reveal that while HPM has significantly distorted the colour. HP Filter followed by HP Fusion and HPM perform best on the fusion of 1:50 resolution ratio. It is to be noted that the filtering techniques have performed better here, than COS. One reason for poor performance of COS is that, IRS PAN sensor wavelength only encompasses MODIS band 3 (B) and 4 (G) part of the EM spectrum (see Figure 5). Since all other MODIS bands do not intersect with the IRS PAN band in the corresponding wavelength region, so the fusion quality of COS has degraded. It is to be noted that these fused images are not very useful for visual assessment of the results.

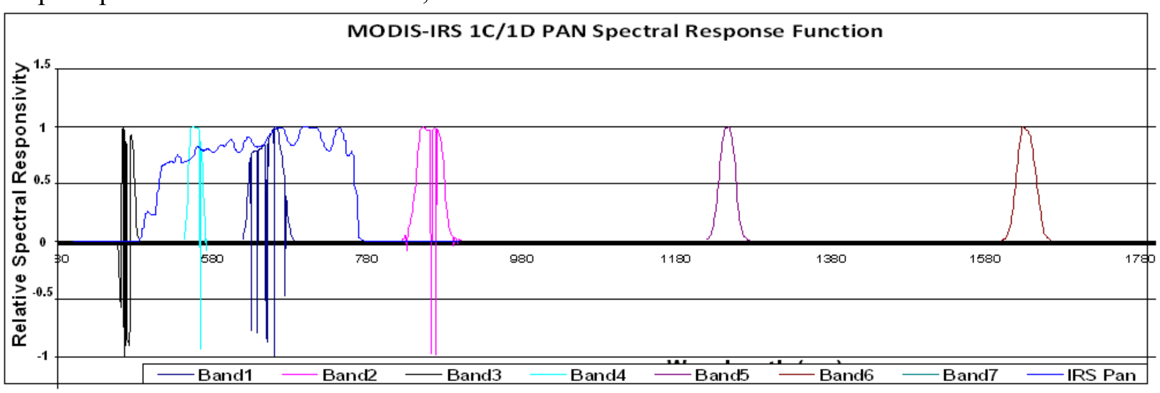

Figure Error! No text of specified style in document.**: Spectral response pattern of IRS 1C/1D PAN-MODIS.**

4.4 Fusion of 1:100 resolution ratio (IRS PAN 5 m + MODIS 500 m)

SRF of IRS 1C/1D PAN and MODIS 7 bands are same as Figure 5. $\overline{C}$, r and $\overline{W}$ are same as in 1:50 resolution ratio (IRS PAN + MODIS 250 m). The original, fused images and statistical properties of the fused bands (not shown here) reveal that SFIM has abrupt change in digital numbers while HPM has greatly distorted the colour in the fused image. HP Filter produced fused images that are closest to the original images.

4.5 Fusion of 1:250 resolution ratio (IKONOS PAN 1 m + MODIS 250 m)

SRF of MODIS 7 bands are as shown in Figure 6.

$C_1 = 0.347241$, $C_2 = 0.387650$, $C_3 = 0.1544$, $C_4 = 0.2172$, $C_5 = 0.3461$, $C_6 = 0.3922$ and $C_7 = 0.4125$; $r = 1.2373$; $\overline{W}$ for IKONOS is ($W_1 = 0.3332$, $W_2 = 0.3300$, $W_3 = 0.3700$, $W_4 = 0.3824$, $W_5 = 0.4838$, $W_6 = 0.5036$ and $W_7 = 0.6093$).

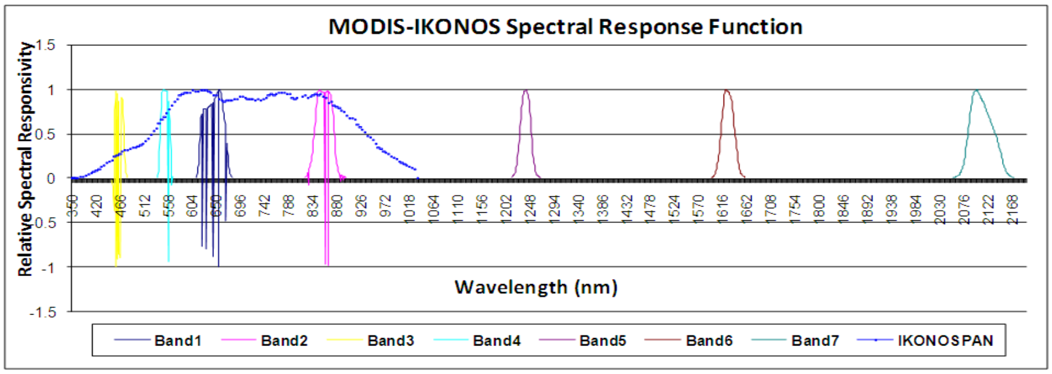

Figure 6: Spectral response pattern of MODIS-IKONOS.

Figure 6 shows that IKONOS PAN band encompasses only MODIS band 1-4 (B, G, R and NIR). Visual appearance of fused images (not shown here) does not bring any sharpness and one may not see significant improvement in the pixel's appearance before and after image fusion. However, statistical properties of the fused images reveal that HP Filter retains all the properties after fusion.

4.6 Fusion of 1:500 resolution ratio (IKONOS PAN 1 m + MODIS 500 m)

SRF of MODIS 7 bands and IKONOS PAN are same as Figure 6. $\overline{C}$, r and $\overline{W}$ are also same as in 1:250 resolution ratio (IKONOS PAN + MODIS 250 m). Although statistical measures reveal that HP Filter is most successful in retaining statistical properties of the original bands, advantages of image fusion with ratio 1:500 are not evident from the fused images. Table 10 summarises the best technique for each resolution ratio. Visual fusion qualities in Table 10 are graded as bad, good and excellent depending upon how clearly the objects could be identified, amount of colour distortion and sharpness of boundaries of objects in the fused images.

From the above study, it may be concluded that fusion of high and moderate spatial resolution MS band with HSR PAN band retains the spatial and spectral properties of the fused bands. However, as the spatial resolution decreases, fusion of images does not facilitate image quality enhancement for object identification. The fusion of multi-sensor data is limited by several factors. Often, lack of simultaneously acquired multi-sensor data hinders successful implementation of image fusion. In case of large differences in spatial resolution of input data, problems arise from limited (spatial) compatibility. Since there is no standard procedure of selecting the optimal data set, the user is often forced to work empirically to find the best result.

Table 10: Optimum fusion technique for various resolution ratios and sensors

Sl. No.	Resolution ratio	Data	Resolution in m	Technique	Visual fusion quality
1	1:4	IKONOS PAN and MS	1 m + 4 m	SFIM	Excellent
2	1:4	IRS PAN and LISS-III MS	6 m + 24 m	HPM	Excellent
3	1:2	Landsat PAN and MS	15 m + 30 m	COS	Excellent
4	1:50	IRS PAN and MODIS	5 m + 250 m	HP Filter	Good
5	1:100	IRS PAN and MODIS	5 m + 500 m	HP Filter	Good
6	1:250	IKONOS PAN and MODIS	1 m + 250 m	HP Filter	Bad
7	1:500	IKONOS PAN and MODIS	1 m + 500 m	HP Filter	Bad

The fusion techniques are very sensitive to mis-registration. In some cases, especially if images of different spatial resolutions are involved, resampling of low resolution image to the pixel size of high resolution image might cause a blocky appearance. Therefore a smoothing filter can be applied before actually fusing the images (Chavez, 1991). The resulting image map can be further evaluated and interpreted related to the desired application.

Once the fused images were obtained, pattern classifiers were used to do the temporal analysis of the status of wetlands in Greater Bangalore as shown in Table 11 and Figure 7. The analyses indicate the decline of 34.48% during 1973 to 1992, 56.90% during 1973-2002 and 70.69% during 1973-2007 in the erstwhile Bangalore city limits. Similar analyses done for Greater Bangalore (i.e. Bangalore city with surrounding 8 unicipalities) indicate the decline of 32.47% during 1973 to 1992, 53.76% during 1973-2002 and 60.83% during 1973-2007.

Table 11: Status of wetlands in Bangalore city limits and Greater Bangalore

	Bangalore City		Greater Bangalore	
	Number of Wetlands	Area (in ha)	Number of Wetlands	Area (in ha)
SOI	58	406	207	2342
1973	51	321	159	2003
1992	38	207	147	1582
2002	25	135	107	1083
2007	17	87	93	918

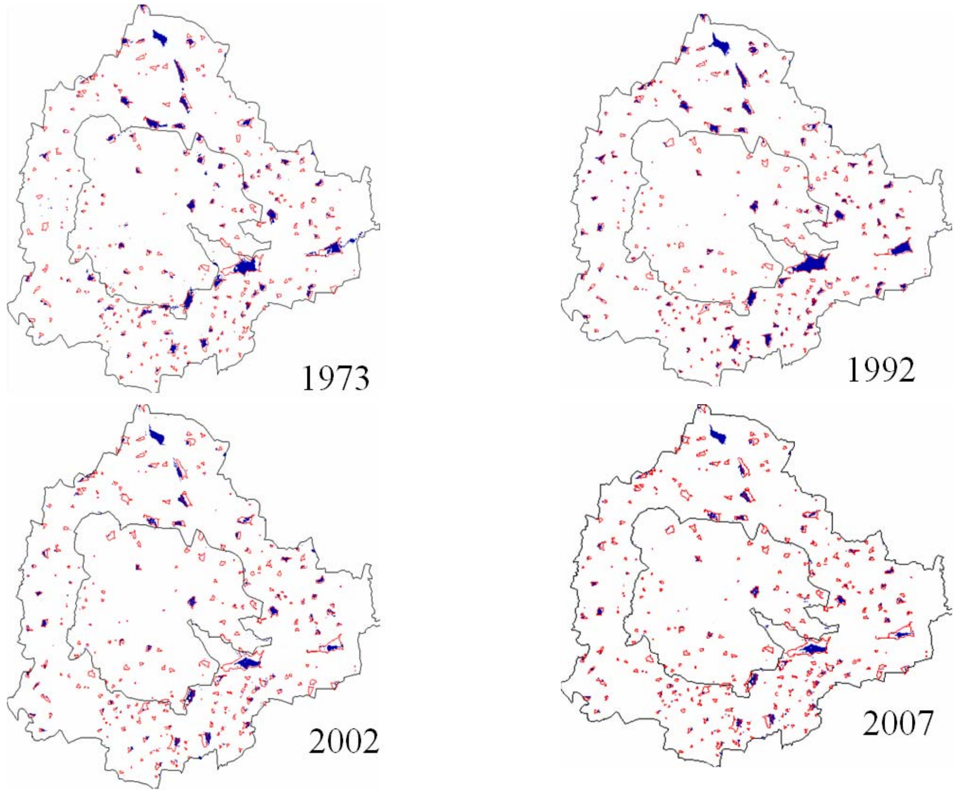

Figure 6: Spatio-temporal analysis of wetlands of Greater Bangalore. Wetlands are represented in blue and the vector layer of wetlands generated from SOI Toposheet is overlaid in red. The inner boundary (in black) is the Bangalore city limits and the outer boundary represents the spatial extent of Greater Bangalore.

There were 159 wetlands spread in an area of 2003 ha in 1973, that number declined to 147 (1582 ha) in 1992, which further declined to 107 (1083 ha) in 2002, and finally there are only 93 wetlands (both small and medium size) with an area of 918 ha in Greater Bangalore region in 2007. Wetlands in the northern part of Greater Bangalore are in a considerably poor state compared to the wetlands in southern Greater Bangalore. Validation of these wetlands were done through field visits during July 2007, which indicate an accuracy of 91%. The error of omission was mainly due to the cover of water hyacinth (aquatic macrophytes) in wetlands due to which the energy was reflected in IR bands rather than getting absorbed. Fifty-four wetlands were sampled through field visits while the remaining wetlands were verified using online Google Earth (http://earth.google.com).

Disappearance of wetlands and a sharp decline in the number of wetlands in Bangalore is mainly due to intense urbanization and urban sprawl. Many lakes were encroached for illegal buildings (54%). Urbanisation and the consequent loss of lakes has led to decrease in catchment yield, water storage capacity, wetland area, number of migratory birds, floral and faunal diversity and ground water table. Studies reveal the decrease in depth of the ground water table from 10-12 m to 100-200 m in 20 years due to the disappearance of wetlands. Field surveys (during July-August 2007) show that nearly 66% of lakes are sewage fed, 14% surrounded by slums and 72% showed loss of catchment area. Also, lake catchments were used as dumping yards for either municipal solid waste or building debris. The areas surrounding these lakes have illegal constructions of buildings and most of the time slum dwellers occupy the adjoining areas. At many sites, water is used for washing and household activities and even fishing was observed at one of these sites. Multi-storied buildings have come up on some lake beds that have totally intervened with the natural catchment flow leading to a sharp decline in the catchment yield and also a deteriorating quality of wetlands. Some of the lakes have been restored by the city corporation and the concerned authorities in recent times. These lakes have a well defined boundary, clean water and are maintained by the neighborhood people. These lakes are used for recreational purposes. They are home to migratory birds and also add aesthetic beauty to the surroundings.

5. CONCLUSION

The study indicated that HPM is most suitable technique for merging IRS MS and PAN images. COS is best for fusing 1:2 Landsat ETM+ PAN and MS bands. HP Filter performed best on the fusion of 1:50 and 1:100 resolution ratio data. Visual appearance of fused images (IKONOS PAN and MODIS, 1:250 and 1:500) did not bring any sharpness and one may not see significant improvement in the pixel's appearance before and after image fusion. However, statistical properties of the fused images revealed that HP Filter retained all the properties after fusion. It may be concluded that fusion of high and moderate spatial resolution MS band with HSR PAN band retains the spatial and spectral properties of the fused bands. However, as the spatial resolution decreases, fusion of images does not facilitate image quality enhancement for object identification. In such cases, spectral unmixing techniques can be employed on low spatial resolution data.

Pattern classifiers along with the advances in geo-informatics coupled with the availability of higher spatial, spectral and temporal resolution data help in extracting spatial features of interest like land cover classes such as wetlands. In this context, an important application of pattern classifiers would be to accurately estimate the spatial extent of temporal wetlands that are useful in monitoring their status. The analysis showed that the number of wetlands declined by 61% in Greater Bangalore. The city administration needs to improvise upon the growth model so that the city caters not only to the growing needs of the population but also restore and maintains the natural assets from further degradation and achieve a sustainable environment.

6. REFERENCES

- Aiazzi, B., Alparone, L., Baronti, S., and Garzelli, A., (2002), Context-driven fusion of high spatial and spectral resolution images based on oversampled multi-resolution analysis. IEEE Transactions on Geoscience and Remote Sensing, vol. 40(10), pp. 2300-2312.

- Bharath, H Aithal, Uttam Kumar, and Ramachandra T. V., (2009), Fusion of multi resolution remote sensing data for urban sprawl analysis, Proceedings of COSMAR 2009, Department of Management Studies, Indian Institute of Science, Bangalore, India, 5-6 November, 2009.
- Chavez, P. S., Sides, S. C., and Anderson, J. A., (1991), Comparison of three different methods to merge multiresolution and multispectral data: TM & SPOT pan. Photogrammetric Engineering and Remote Sensing, vol. 57, pp. 295-303.
- Kevin, W., & El Asmar, H. M. (1999). Monitoring changing position of coastlines using thematic mapper imagery, an example from the Nile Delta. Geomorphology, 29(1), 93-105.
- Kumar, U., Mukhopadhyay, C., and T. V. Ramachandra, (2009a), Pixel based fusion using IKONOS imagery. International Journal of Recent Trends in Engineering (Computer Science), vol. 1, no. 1, pp. 173-177.
- Kumar, U., Mukhopadhyay, C., and Ramachandra T. V., (2009b), Fusion of Multisensor Data: Review and Comparative Analysis, Proceedings of the 2009 WRI Global Congress on Intelligent Systems, 19-21 May 2009, Xiamen, China, vol. 2, pp. 418 – 422, IEEE Computer Society, Conference Publishing Services, Los Alamitos, California.
- Kumar, U., Dasgupta, A., C. Mukhopadhyay, N. V. Joshi, and Ramachandra T. V., (2011), Comparison of 10 Multi-Sensor Image Fusion Paradigms for IKONOS images. International Journal of Research and Reviews in Computer Science, Academy Publisher, United Kingdom, vol. 2, no. 1, pp. 40-47.
- Ramachandra, T.V., Kiran, R., & Ahalya, N. (2002). Status, conservation and management of wetlands. New Delhi: Allied Publishers.
- Ramachandra T. V., and Kumar, U., (2008), Wetlands of Greater Bangalore, India: Automatic Delineation through Pattern Classifiers. The Greendisk Environmental Journal, (International Electronic Journal), vol. 1, no. 26, pp.1-22.
- Wang, D., Ziou, C., Armenakis, Li, D., and Li, Q., 2005, A Comparative Analysis of Image Fusion Methods. IEEE Transactions of Geoscience and Remote Sensing, vol. 43(6), pp. 1391-1402.